Fast Transient Tests: Trivial or Terminal Pursuit ?

François D. Martzloff and Perry F. Wilson
National Bureau of Standards
f.martzloff@ieee.org

Reprinted, with permission, from
Proceedings, 7th International Zürich Symposium on Electromagnetic Compatibility, 1987

Significance:
Part 4 – Propagation and coupling of surges

In the early 80's, considerable interest arose in developing an IEC standard test method to assess the immunity of electronic equipment against "fast transients" such as those that can be produced by contact bouncing in power circuits. Such transients could propagate from their source – the bouncing contact – to the power port of equipment, or be coupled by proximity into control cables connected to the equipment of interest. The issue was not so much the potential for damaging the equipment – as in surge occurrences – but rather the possibility of disturbing proper operation of the equipment.

Motivated by some skepticism on how far such fast transients can propagate, measurements, augmented by theoretical numerical simulations were conducted on representative power wiring configurations. The findings, showing good agreement between theory and experiments, validated the expectation, that is, substantial attenuation occurs when these fast transients travel more than a few tens of meters away from their source. See also file "Propag EFT2 1990" for additional tests on a variety of cable configurations.

This paper was recognized by the EMC Symposium award.

FAST TRANSIENT TESTS - TRIVIAL OR TERMINAL PURSUIT ?

François D. Martzloff
Electrosystems Division
National Bureau of Standards
Gaithersburg, MD 20899

Perry F. Wilson
Electromagnetic Fields Division
National Bureau of Standards
Boulder, CO 80303

SUMMARY

Measurements, augmented by theoretical simulation techniques, have been performed to determine the attenuation of fast transients propagating in typical indoor (conduit-enclosed) power lines. The rise time of the applied pulses ranges from 0.7 to 50.0 ns, including the International Electrotechnical Commission (IEC) 5/50 ns pulse recently recommended for fast transient tests. Theory and measurements confirm that pulse amplitude attenuation increases significantly for shorter pulses. For comparison and validation of the theoretical model, the IEC pulse was also applied to a conventional coaxial cable.

INTRODUCTION

Surge testing requirements are of increasing interest among manufacturers and users of electronic equipment. Performance progress is often obtained with fast logic devices which can be quite sensitive to external overvoltages, both amplitude and rate of change. The operation of electronic equipment in potentially hostile environments mandates realistic surge testing in order to better understand failure modes and to validate advanced protection schemes.

Existing standards such as those of the IEC, IEEE, and ANSI require surge test waveforms with rise times generally longer than 100 ns [1]-[3]. However, recent proposals [4]-[5] advocate fast-transient tests with waveforms representative of electrostatic discharge events or relay contact bounces. The rationale for such proposals is based on an increased awareness of the significance of fast transients. This awareness results from two factors; (1) increases in the bandwidth and writing speed of oscilloscopes which reveals the characteristics of these phenomena, and (2) unexplained field failures of equipment which pass conventional surge tests.

There is a risk that unrealistic emphasis might be placed on these steep-front waves. Their occurrence and effect on nearby equipment have been documented. However, the propagation characteristics of power and (some) data lines might produce fairly rapid attenuation of the high frequency components of these fast transient surges. Comprehensive data on surge attenuation at these frequencies have not been published to our knowledge. Thus, quantitative laboratory tests, augmented by theoretical simulation techniques, should contribute to better decisions on the importance and applicability of proposed fast-transient standards, as well as complement previous studies on surge propagation involving lower frequencies [6]. The experimental (Martzloff) and theoretical (Wilson) portions of this investigation were performed independently by the two authors. The results are compared in this paper.

EXPERIMENTAL CONFIGURATION AND SIMULATION

A representative low-voltage, indoor, single-phase power line with three conductors in a steel conduit was set up in a laboratory. A length of 63 m was selected (20 standard conduit sections). The line was built with normal industrial components and practices but in a zig-zag pattern with both ends at essentially the same location. This allowed both send and receive measurements to be performed with the same instrumentation and without physically moving any equipment. Three insulated (600 V), stranded-copper conductors of # 14 AWG (1.6 mm diam.) were pulled in a steel conduit (20 mm diam.) and connected as shown in Figure 1. At the sending end, the neutral conductor is bonded

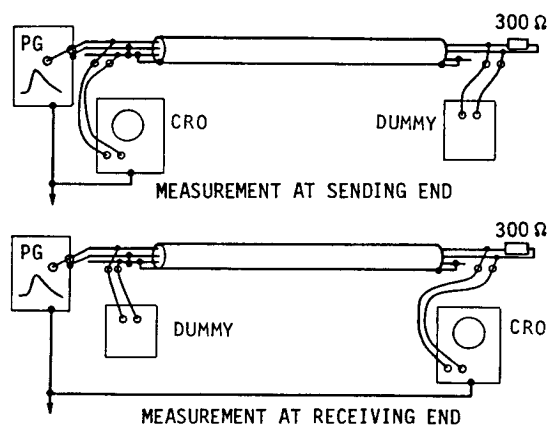

Fig. 1. Connection of conductors and instrumentation for the measurement of attenuation of steep-front pulses in a conduit line.

to the grounding (safety) conductor and to the conduit. At the receiving end, the neutral wire was not bonded to the grounding conductor or conduit. This type of connection is typical U.S. practice for a branch circuit originating at a service entrance.

A family of fast surges, ranging from 0.7 to 50 ns in rise time and of duration three times the rise time were generated for propagation along the line. The IEC EFT (Electrical Fast Transient) pulse of 5/50 ns was also used as an input signal. For a baseline comparison, a 63 m length of conventional RG58 coaxial cable was also subjected to the IEC EFT pulse. Details of the instrumentation are given in Appendix A.

Pulse propagation on a transmission line depends on the pulse shape (rise time, width, frequency content, etc.) and the transmission-line characteristics (geometry, materials, etc.). The analysis of the pulse propagation follows the previous work of Wingington and Nahman [7]. The transmission line characteristics for various lines will be primarily derived from King [8]. The details are left to Appendix B. The general problem of multiconductor lines within a circular conduit is beyond the scope of this paper. Thus, we consider a coaxial line, which models the RG58 cable, and a pair of wires symmetrically located within a conduit (see Fig. B2). This latter case neglects the grounding conductor in the actual experimental setup but is a reasonable idealization of the power-line configuration. These transmission lines are assumed to be uniform. In practice, the location of the inner conductors may vary within the conduit due to sag, bends, and so forth. Thus, we consider two special cases; (1) wires near the center separated only by the thickness of the wire insulation, and (2) wires near the wall of the conduit again to within the thickness of the wire insulation. Because the insulation has a higher dielectric constant than does air, its presence will increase the attenuation of the surges. However, the insulation thickness about each wire is small and for simplicity their effect is ignored.

EXPERIMENTAL RESULTS

Figure 2 shows composite oscillograms of the pulse applied at the sending end and arriving at the receiving end for a family of four unidirectional pulses with comparable duration/rise-time ratios. We find substantial attenuation (97%) for the fastest pulse (0.7-ns rise time), and still appreciable attenuation (40%) for the slowest pulse (50-ns rise time). In addition to the attenuation of the peaks, the rise time of the pulse is increased at the far end, with a stretching of the duration, sometimes referred to as 'smearing the pulse'. The oscillograms for each type of pulse also show that while the peaks are attenuated, the integrals of the voltages with respect to time of the pulses at the sending and receiving ends are comparable. This last observation implies that equipment sensitive to peaks or to steep fronts will be somewhat protected by a line of sufficient length. However, if the equipment is sensitive to energy, the presence of the line will not significantly decrease its exposure.

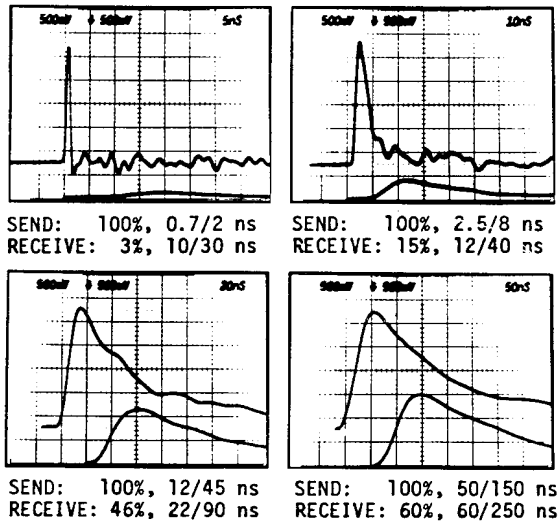

Fig. 2. Composite oscillograms of sending-end and receiving-end pulses for four pulses of increasing rise time duration in the 63-m conduit line.

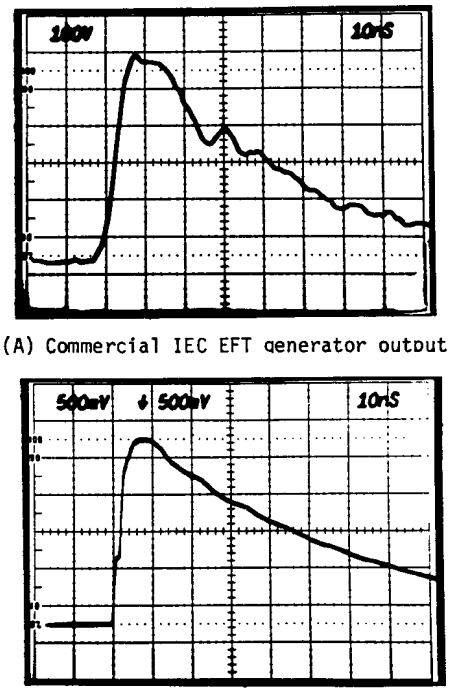

(A) Commercial IEC EFT generator output

(B) NBS pulse-forming circuit output

Fig. 3. Typical waveforms in accordance with IEC EFT requirements.

The IEC is currently developing a requirement for EFT tests with a repetitive burst of pulses [5], each having a 5-ns rise time and a 50-ns duration above 50% of the peak value. This type of transient is typical of local switching of loads which potentially can be coupled into adjacent power or data lines. Commercial generators are now available for simulating these transients with preset amplitudes in the range of 0.5 to 4.0 kV. An example is shown in Figure 3A. For more repeatable waveforms in this study, such as shown in Figure 3B, a 5/50-ns pulse of

lower voltage was obtained by discharging a 1-nF capacitor through a mercury-wetted relay into 20 m of RG58 cable. Furthermore, the lower voltage pulse allowed direct connection into the 50-Ω, 10-V maximum input of the preamplifiers, instead of requiring an attenuator with attendant effect on the rise-time response (see the artificially smooth rise of the trace on Fig. 3A). Figure 4 shows the sending-end and receiving-end oscillograms for this idealized pulse waveform for 25, 38, and 63-m lengths in the conduit line.

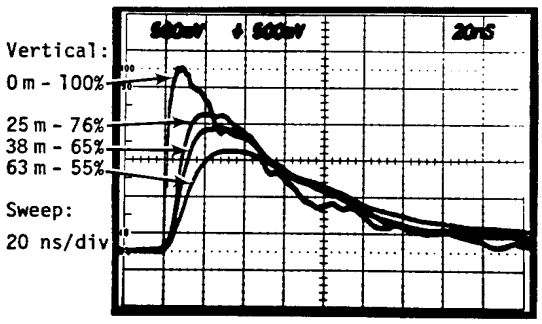

Fig. 4. Sending-end and receiving-end oscillograms for the IEC EFT pulse in 25, 38, and 63-m lengths of conduit line.

Finally, a comparable length of RG58 coaxial cable was also subjected to the same measurements with the 5/50-ns pulse. Figure 5 shows the results. The expected lesser attenuation, compared to that of the power line, is quite apparent. Coaxial cables are intended to provide a minimum attenuation of high frequency signals. A slightly slower propagation speed due to the solid dielectric of the coaxial cable was noticed, in contrast with the composite solid-air dielectric of the conduit line.

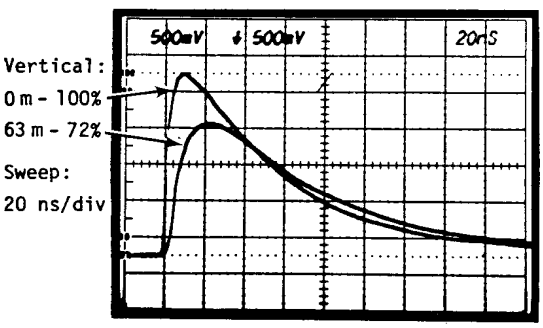

Fig. 5. Sending-end and receiving-end oscillograms for the IEC EFT pulse in 63 m of RG58 coaxial cable.

THEORETICAL SIMULATION RESULTS

Table I summarizes the results obtained from the analytical model and experimental measurements. In the theoretical approach, there is a marked difference between results for the two model cases (wires near center or conduit wall) as might be expected. For comparison with the experimental results, an intermediate value between the two limiting cases should be selected. The combined effect of gravity and residual curvature of the conductors pulled from a spool may place the conductors against the wall. Therefore, the actual configuration should give results similar to those of the theoretical case with the wires near the wall. Indeed, these agree within ±16% for the various pulses.

Figure 6 shows simulated results for the IEC EFT pulse in the 63 m conduit line. The input pulse is approximated from Figure 4 with linear splines (* curve, see Appendix, eq. B5). The resulting output pulses (eq. B10) for the two-wire configurations are shown. For comparison, an approximation to the actual measured output pulse (Fig. 4) is also included. The measured pulse lies between the two special cases, with the wires-near-conduit curve better predicting the measured pulse as expected. Qualitatively, the theoretical pulses look very much like the measured pulses. We can in fact choose the model parameter k (= 0.000114) such that attenuation for the 63 m line is accurately matched. Given this empirically determined value we, then consider the effect of varying the line

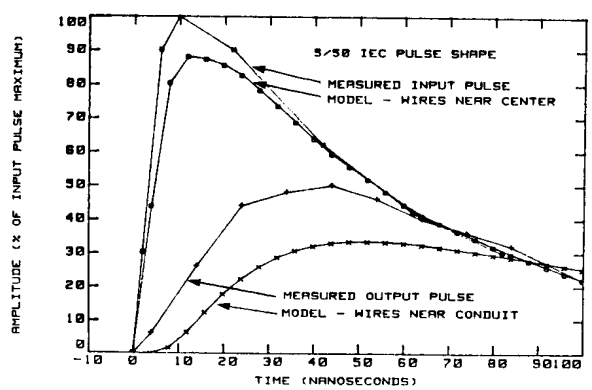

Fig. 6. Sending-end and receiving-end curves for the IEC EFT pulse in the 63-m conduit line. Both theoretical curves and linear approximations to the measured data are shown.

Table I
Comparison of theoretical prediction and experimental results

sending-end / receiving-end	ns pulses in conduit				5/50 ns IEC pulse	
	0.7/2	2.5/8	12/45	50/150	conduit	coax
Attenuation (%)						
Theoretical Model						
wires → conduit center	45	26	12	6	12	25
wires → conduit walls	99	92	68	50	66	N/A
Measured Results	97	85	54	40	45	25
Rise Time (ns)						
Theoretical Model						
wires → conduit walls	10	11	22	70	30	12
Measured Results	10	12	22	60	30	14

length. The results are depicted in Figure 7. Measured data show maximum amplitudes of 76% and 65% for the 25 and 38 m line lengths. The predicted amplitudes (Fig. 7) are 75% and 67% respectively, and thus are in good agreement. Also shown are the predicted pulse shapes for 120 and 240 m lengths with the expected continued attenuation and smearing of the pulse.

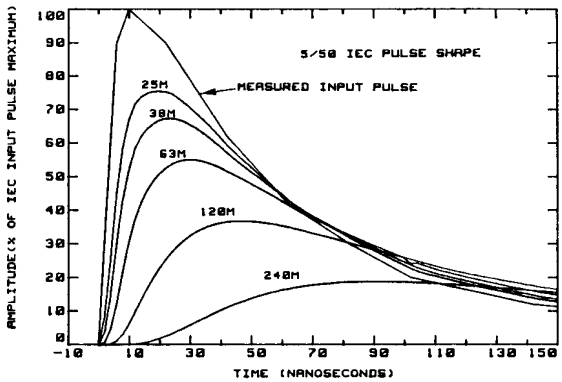

Fig. 7. Attenuation for the IEC EFT pulse in representative conduit line as a function of line length.

Figure 8 shows results for the 63-m length of RG58, again for the IEC EFT pulse. The input and output linear approximations are taken from the waveforms in Figure 5. The results of the theoretical model agree very well with the measured data. This is expected since in this case the transmission line cross section is uniform and the line parameters are well defined.

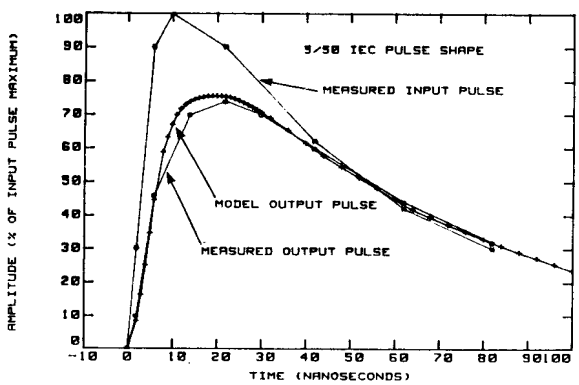

Fig. 8. Sending-end and receiving-end curves for the IEC EFT pulse in 63 m of RG58 coaxial cable.

CONCLUSIONS

1. Theoretical modeling based on a physical description of the line parameters yields results which agree with laboratory measurements, even for steep-front surges such as those currently proposed by new standards.

2. These steep-front surges suffer appreciable attenuation when propagating in power lines. Both amplitude and steepness of the surge front are reduced, with steep, short pulses affected more than longer pulses.

3. This attenuation will be a welcome mitigating effect for load equipment connected at the end of a long line and not exposed to transients generated by nearby equipment.

4. The attenuation is greater for steepness and amplitude than for the voltage-time integral of the surge. This suggests that dispersion dominates wall losses in reducing the pulse maximum. Therefore, this attenuation will benefit equipment sensitive to noise interference more than those sensitive to energy interference.

5. Coaxial cable, as opposed to a power line made of wires somewhat randomly located in a steel conduit, produces far less attenuation. The model-measurement correlation is improved because the coaxial-cable geometry is well defined.

APPENDIX A - INSTRUMENTATION

Voltages were recorded with a Tektronix 7104 (* see refs.) oscilloscope provided with two 7A29 (* see refs.) vertical amplifiers. The mainframe of the oscilloscope performed the differential combination of the two signals. In this configuration, the bandwidth of the system is only 500 MHz, compared to the 1 GHz capability of the single-ended measurement with only one amplifier. This reduction in performance is an acceptable trade off to obtain the differential connection while the conduit, oscilloscope chassis and low side output of the generator are bonded together, and hence assure minimum noise coupling. Where high voltages are involved, this configuration provides improved safety. This was not a concern here as the measurement on this linear system were conducted with signals in the 5-V range. A check on the common mode rejection of the system indicated less than 5% residual signal, an insignificant effect compared to the attenuation levels measured.

The amplifiers have a 50-ohm input impedance, so that the effective impedance of the differentially connected probe is 100 ohms. To make the measurements at the sending end, the voltages of the line and neutral conductors with respect to chassis ground were each fed to one of the preamplifiers. In this manner, the pulse delivered by the generator impinges on an impedance consisting of the two amplifiers in series and in parallel with the line. To make measurements at the receiving end, the same oscilloscope was used, with the same connection. However, the pulse arriving at the receiving end would experience a reflection due to any impedance mismatch. To obtain an impedance match, time-domain reflectometry was used to trim the terminating load until no reflection occurred. Good matching was obtained with a 75-ohm termination. With the two conductors isolated from the conduit, but still contained in the conduit, the characteristic impedance determined by this method was 280 ohms, typical of a twin-conductor line. With the 100-ohm impedance of the probe, a 300-ohm parallel resistance at the line end brought the termination to 75 ohms, avoiding mismatching enhancements or attenuation at the line end.

A dummy was constructed to provide the same matching impedance as that of the oscilloscope-probe combination (see Fig. 1). When recording the receiving-end waveforms with the oscilloscope, the dummy was connected in parallel with the line at the sending end. Thus, the impinging pulse from the generator would be presented the same load impedance as during measurements at the sending end.

APPENDIX B - THEORETICAL MODEL

A uniform line may be characterized by a series impedance $Z(s)$ and shunt admittance $Y(s)$ where s is the Laplace transform variable. These in turn depend on the internal impedance $R(s)$ (internal resistance and inductance), the (static) external inductance L, the (static) capacitance C, and the conductance $G(s)$ of the material filling the transmission line [7] $Z(s) = R(s) + sL$ and $Y(s) = G(s) + sC$. We define the transmission-line characteristic impedance $Z_0(s)$ and propagation function $\gamma(s)$ in the usual fashion. Most transmission lines, including those of interest here, are filled with a nearly lossless material. This implies that $G(s) \approx 0$. For a well designed, practical transmission line the series internal resistance should also be relatively small, even at higher frequencies. Making this assumption allows us to expand $Z_0(s)$ and $\gamma(s)$ in terms of a Taylor series in $R(s)$. We will retain only the first order loss perturbation term which yields

$$Z_0(s) \approx Z_0 + \frac{1}{2}\frac{R(s)}{s\gamma_0}, \text{ and}$$
$$\gamma(s) \approx s\gamma_0 + \frac{1}{2}\frac{R(s)}{Z_0}, \tag{B1}$$

where Z_0 and γ_0 are the usual loss-free values associated with the line. These approximations appear in the paper by Wingington and Nahman [7].

Consider the generic transmission line of length ℓ shown in Figure B1 which will serve to model the experimental line depicted in Figure 1. It is excited by a generator voltage $V_g(s)$, with a generator impedance $Z_g(s)$, and terminated in a load impedance $Z_t(s)$. We are interested primarily in comparing the voltage appearing at the input end $V_i(s)$ to the voltage received at the output $V_o(s)$. We find that

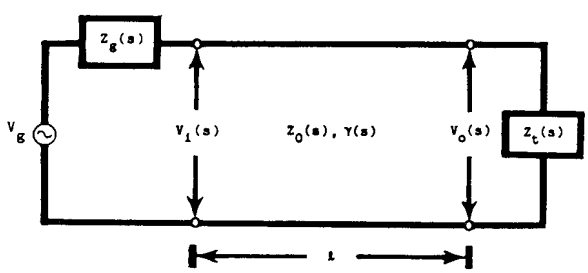

Fig. B1. Transmission line model of surge propagation experiment.

$$\frac{V_o(s)}{V_i(s)} = 2\left[\frac{Z_t(s)}{Z_0(s) + Z_t(s)}\right]\left[\frac{e^{-\gamma(s)\ell}}{1 + \Gamma_r(s)e^{-2\gamma(s)\ell}}\right],$$
$$\Gamma_r(s) = \frac{Z_t(s) - Z_0(s)}{Z_t(s) + Z_0(s)}. \tag{B2}$$

Substituting (B1) into (B2) will yield an approximate form for the voltage ratio of interest; however, we need not be so general. For this analysis we may assume that the line is terminated in a resistive load equal to the lossless characteristic impedance of the line, that is $Z_t(s) = Z_0$. Further, if the resistive contribution at high frequencies is small compared to the characteristic impedance, the reflection terms in (B2) do not contribute. Combining results we find that the output voltage may be written in terms of the input (to the line) voltage as

$$V_o(s) \approx V_i(s)\, e^{-s\gamma_0\ell}\, A(s), \text{ and}$$
$$A(s) \approx e^{-R(s)\ell/2Z_0}, \tag{B3}$$

where $A(s)$ represents the attenuation due to line losses. In other words, we will consider the line to be well matched, consistent with the experimental procedure. The term $\exp(-s\gamma_0\ell)$ is simply the lossless case propagation delay due to the line length ℓ.

We may now make use of Laplace transform properties to find $v_o(t)$ given $v_i(t)$. The inverse Laplace transform of the receiving-end voltage is given by

$$v_o(t) = \{v_i(t-\gamma_0\ell) * a(t-\gamma_0\ell)\}\, u(t-\gamma_0\ell), \tag{B4}$$

where the lower case symbols represent the respective inverse Laplace transforms, * denotes a convolution integral, and $u(t)$ is the unit step function at $t = 0$.

The input voltage is typically not given in analytical form. Thus, for simplicity we will use a series of linear functions $r_n(t)$ to approximate $v_i(t)$. The function $r_n(t)$ is simply a ramp rising from zero at time t_n to a value a_n at time t_{n+1}, and then remaining at this level for $t \geq t_{n+1}$. By using a combination of these, with positive and negative slopes, we may approximate a given pulse. That is, we let

$$v_i(t) \approx \sum_{n=0}^{N} r_n(t). \tag{B5}$$

This form may be used to evaluate the convolution integral (B4) being careful to use the proper expression for $r_n(t)$ over the various time intervals.

The attenuation function $a(t)$ requires that we specify $R(s)$ and Z_0. It is worthwhile to first examine the relatively simple case of a circular coaxial line with central inner conductor. We then will look at a pair of conductors within a conduit. Let the inner

and outer coaxial conductor radii be designated a_1 and a_2. This type of line may be readily analyzed with the result that [8]

$$Z_0 = 60\varepsilon_r^{-1/2}\ln(a_2/a_1), \text{ and} \tag{B6}$$

$$R(s) \approx Ks^{1/2} = \frac{1}{2\pi}\left[\frac{1}{a_1}\left(\frac{\mu_0}{\sigma_1}\right)^{1/2}+\frac{1}{a_2}\left(\frac{\mu_0}{\sigma_2}\right)^{1/2}\right] s^{1/2},$$

where ε_r is the relative permittivity of the material filling the coaxial line, all materials are assumed to have a permeability μ_0, σ_1 and σ_2 are the conductivity of the inner and outer conductors, and K simply denotes the terms preceeding $s^{1/2}$ for convenience. The expression for R(s) is a high-frequency approximation for two wires with uniform current distributions. From Laplace transform tables we find that

$$a(t) = \frac{k}{2}\pi^{-1/2}t^{-3/2}e^{-k^2/4t}, \tag{B7}$$

where we have let $k = K\ell/2Z_0$. Substituting in (B5) for $v_i(t)$ and (B7) for a(t) yields

$$v_i(t)*a(t) = \frac{k}{2}\pi^{-1/2}\sum_{n=0}^{N} g_n(t), \tag{B8}$$

where for $t < t_n$ $g_n(t) = 0$, for $t_n \le t \le t_{n+1}$

$$g_n(t) = \frac{a_n}{\Delta_n}\{\Delta t_n I(\tfrac{3}{2},\Delta t_n) - I(\tfrac{1}{2},\Delta t_n)\},$$

and for $t_{n+1} \le t$ (B9)

$$g_n(t) = a_n I(\tfrac{3}{2},\Delta t_{n+1}) + \frac{a_n}{\Delta_n}\{\Delta t_n[I(\tfrac{3}{2},\Delta t_n) - I(\tfrac{3}{2},\Delta t_{n+1})] - I(\tfrac{1}{2},\Delta t_n) + I(\tfrac{1}{2},\Delta t_{n+1})\},$$

where $\Delta_n = t_{n+1} - t_n$, $\Delta t_m = t - t_m$, and

$$I(\tfrac{3}{2},a) = \frac{2}{k}\pi^{1/2}\operatorname{erfc}(\tfrac{k}{2}a^{-1/2}), \text{ and}$$

$$I(\tfrac{1}{2},a) = 2a^{1/2}e^{-k^2/4a} - \tfrac{1}{2}k^2 I(\tfrac{3}{2},a).$$

Collecting results we find that

$$v_o(t) = \frac{k}{2}\pi^{-1/2}\sum_{n=0}^{N} g_n(t-\gamma_0\ell). \tag{B10}$$

A coaxial line is simple to analyze, but it does not model well the power-line conduit configuration. A more realistic idealization is the shielded pair line shown in figure B2. Although it ignores the third grounding wire and the effects of wire insulation, it should provide reasonable results. The model assumes that the line is driven in a balanced configuration with the two inner conductors in series carrying equal and opposite currents. The two inner conductors have radius a_1 and are separated by a distance 2D, and the outer sheath has a radius a_2. We also assume that the inner conductors are removed from the sheath sufficiently that we may ignore proximity effects. This requires that $a_2^2 - D^2 \gg a_1^2$. This condition is met in our modeled results due to the assumed insulation thickness, even for the case of wires near the wall. The internal impedance will consist of the two inner conductor impedances in series, similar to (B6) except that now the conductors have equal radii, plus the impedance of the outer shield which carries anti-symmetric currents on each side. We find that [8]

$$Z_0 = 30\,\varepsilon_r^{-1/2}\ln\left[\frac{2D(a_2^2 - D^2)}{a_1(a_2^2 + D^2)}\right], \text{ and} \tag{B11}$$

$$R(s) = \frac{1}{\pi}\left[\frac{1}{a_1}\left(\frac{\mu_0}{\sigma_1}\right)^{1/2}+\frac{4}{a_2}\left(\frac{\mu_0}{\sigma_2}\right)^{1/2}\frac{(D/a_2)^2}{1-(D/a_2)^2}\right]s^{1/2}.$$

The remaining analysis is the same as in the symmetric coaxial case with K defined as in (B6).

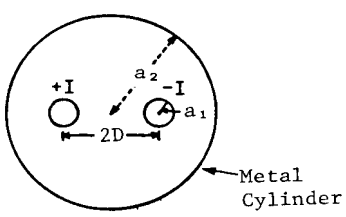

Fig. B2. Shielded pair line.

REFERENCES

[1] IEC Report 664, "Insulation coordination within low-voltage systems, including clearances and creepage distances for equipment," 1980.

[2] ANSI/IEEE C62.41, "IEEE guide for surge voltages in low-voltage ac power circuits," 1980.

[3] ANSI/IEEE C37.90a, "IEEE guide for surge withstand capability (SWC)," 1983.

[4] IEC Standard 802-2, "Electromagnetic compatibility for industrial-process measurement and control equipment - electrostatic discharge requirements," 1984.

[5] IEC Standard 802-4, "Electrical fast transient requirements," Draft.

[6] F. D. Martzloff, and H. A. Gauper, "Surge and high-frequency propagation in industrial power lines," IEEE Trans. Ind. Appl., vol. IA-22, pp. 634-640, July/Aug. 1986.

[7] R. L. Wingington, and N. S. Nahman, "Transient analysis of coaxial cables considering skin effect," IRE Proc., vol. 45, no. 2, pp. 166-174, Feb. 1957.

[8] R. W. P. King, Transmission-line Theory, McGraw-Hill, New York, NY, Ch. 1, 1955.

* Certain commercial instruments are identified in this paper in order to adequately specify the experimental procedure. Such identification does not imply recommendation or endorsement by the National Bureau of Standards, nor does it imply that the instruments identified are necessarily the best available for the purpose.